Journal of Hazardous Materials 172 (2009) 256–261

Contents lists available at ScienceDirect

Journal of Hazardous Materials

journal homepage: www.elsevier.com/locate/jhazmat

A new coral structure TiO_2/Ti film electrode applied to photoelectrocatalytic degradation of Reactive Brilliant Red

Xiao-She Hua, Yi-Jie Zhang, Nai-Heng Ma, Xian-Feng Li, Hao-Wei Wang*

Institute of Ecological and Environmental Materials, School of Environment and Engineering, Shanghai Jiao Tong University, Shanghai 200240, PR China

ARTICLE INFO

Article history:
Received 6 March 2009
Received in revised form 19 June 2009
Accepted 30 June 2009
Available online 8 July 2009

Keywords:
Photoelectrocatalysis
TiO_2
Coral structure
Reactive Brilliant Red

ABSTRACT

A novel structure TiO_2/Ti film was prepared on a titanium matrix using anodic oxidation technique and applied to degrade Reactive Brilliant Red (RBR) dye in simulative textile effluents. The film was characterized by Field-Emission Scanning Electron Microscope (FE-SEM), Laser Micro-Raman Spectrometer (LMRS), UV–vis spectrophotometer (UVS) and Photoelectrocatalytic (PEC) experiment. The results show that the surface morphology of the film is coral structure, and the crystal structure of the film is anatase. The absorbency of the coral structure TiO_2/Ti film is 87–93% in the UV light region, and 77–87% in the visible light region. PEC experiment indicates that the photocurrent density of the coral structure TiO_2/Ti film electrode achieves 160 $\mu A/cm^2$. The color and Chemical Oxygen Demand (COD) removal efficiencies of RBR achieve 73% and 60% in 1 h, respectively. These are 16% and 58% higher than those of nanotube TiO_2/Ti film electrode. These were attributed to that these electrodes with different surface morphologies exhibit distinct surface areas and light absorption rate.

1. Introduction

Reactive dyes are widely used in textile industries owing to their wide variety of color shades, high wet fastness profile, ease of application and brilliant colors [1]. In textile industry, it was estimated that about 10–15% of dyes were lost during the dying process and released as effluents [2]. These effluents are highly colored and can heavily contaminate water source if they are discharged into natural and domestic water systems including rivers, lakes and public sewage without any treatment. More and more concerns are focused on the toxicity and potential toxicity of dye and their precursors. Many techniques are developed to treat the colored water such as physical adsorption [3], H_2O_2-based oxidation [4], catalytic ozonation [5], photocatalysis [6,7], ultrasonic irradiation [8], and electrochemical oxidation [9]. In these techniques, TiO_2 photocatalysis is one of the most promising techniques due to its high photocatalytic activity, stable, low-cost, non-toxic and wide band gap energy.

Since Fujishima and Honda [10] published a paper about TiO_2 electrode splitting water into hydrogen and oxygen under UV lamps in 1972, the TiO_2 photochemical catalysis behaviors have been a subject of extensive research interest. For TiO_2 photocatalyst, the electrons in the semiconductor are excited from the valence band into the conduction band under UV irradiation, resulting in generating the electron–hole pairs. The positive holes are powerful oxidants to degrade the organic compounds [11]. TiO_2 nano-powders due to their high-activity have been used to wastewater degradation. The disadvantages of this kind of materials are that the recombination of hole and electron can be occurred easily, which will reduce the efficiency of catalyst. Moreover, recycle of TiO_2 nano-powders from water is very difficult when they are applied on the sewage treatment in suspension. Simultaneous, the water will be contaminated by the TiO_2 nano-powders if they are not completely separated from water.

To solve these problems, many immovable TiO_2 photocatalyst techniques had been successfully fabricated on some carriers, such as glass, ceramics, zeolite [12–14]. The results from these reports showed that these immovable methods would reduce photocatalyst surface areas and photocatalytic activity. Many efforts have been made to improve the photocatalytic capability of TiO_2 film by using various techniques including noble metal deposition [15,16], cation doping [17], nonmetal doping [18], and coupled semiconductor oxide [19]. Some researchers tried to enlarge the surface areas of TiO_2 film electrode by changing its structures [20–23] such as microporous (volcano-like) [24], nanoporous TiO_2 thin-film [25] and nanotube [26]. These results show that the surface morphology of the TiO_2 film imposes significant influences on its catalytic effect due to the different surface areas and the corresponding photoabsorbency of these different morphologies.

Besides, Ward and Bard [27] reported that the catalytic effect of TiO_2 film could be improved by applying a potential bias to drive the photo-generated electrons via an external circuit and prevented the

* Corresponding author. Tel.: +86 21 34202540; fax: +86 21 34202540.
E-mail address: hwwang@sjtu.edu.cn (H.-W. Wang).

0304-3894/$ – see front matter © 2009 Elsevier B.V. All rights reserved.
doi:10.1016/j.jhazmat.2009.06.166

rapid recombination of electrons and holes, which is the principle of photoelectrocatalytic (PEC) oxidation where the conductance of the carriers is needed.

Presently, much work had been done to improve photocatalytic activity via increasing photoabsorbencies and photo-conversion efficiency. Nevertheless, the activity of TiO_2 film is still to be enhanced to satisfy the demand of its application on wastewater treatment.

A light trapping structure will increase the rate of absorption, subsequently may improve the photocatalytic efficiency. In this work, to investigate the effect of materials with light trapping structure on the photo-conversion and photoabsorbencies, a kind of coral structure TiO_2/Ti film was prepared on the surface of titanium matrix by anodic oxidation technique [28]. Field-Emission Scanning Electron Microscope (FE-SEM) and PEC were used to investigate its structure and photocatalytic characteristics, respectively.

2. Experimental

2.1. Preparation of TiO_2 film electrodes

Titanium sheets (99.6% purity, 80 mm × 80 mm × 1.5 mm) were purchased from Shanghai Hongtai Metal Production Co. Ltd. (Shanghai, China) and employed as the substrates for TiO_2 film coatings. All chemicals (Shanghai Chemical Reagent Co., Ltd., Shanghai, China) were of reagent grade or better quality. All solutions were prepared using doubly distilled water. After polished with 1000 grit sandpaper, the titanium sheets samples were immerged into mixed solution which contains 50 g/L NaOH, 30 g/L Na_3PO_4, and 30 g/L Na_2CO_3 under ultrasonic vibrated for 3 min at 80 °C to degrease, and then immerged into 200 g/L HNO_3, 4 g/L HF mixed solution under ultrasonic vibrated for 3 min at 20 °C to remove oxide layer. Anodic oxidation was carried out in the 1000 mL beaker at 20 °C for 30 min, with the sample being the anode, and a graphite plate (80 mm × 80 mm × 1.5 mm) being the cathode, and 0.5 wt.% HF acid being the electrolyte. The adopted voltage was 20 V and the current density was 0.16 A/dm^2. The sample was cleaned by distilled water after anodic oxidation, and then calcined in a high temperature sintering furnace at 500 °C for 1 h. To compare with this sample, a nanotube and flat TiO_2 film electrodes were also prepared by anodic oxidation method and sol–gel method on the Ti sheets, respectively. The process parameters used in this work are the same as those in the literatures [26,29]. Finally, these electrodes were also calcined in a high temperature sintering furnace at 500 °C for 1 h.

2.2. Characterization of the TiO_2 film electrodes

The surface morphology of these TiO_2 film electrodes was characterized by FE-SEM (FEI SIRION 200 SEM; FEI Corporation; USA). The crystal structure of these TiO_2 film electrodes was confirmed by Raman spectra analysis using a Laser Micro-Raman Spectrometer (LMRS; λ = 514 nm; InVia&Reflex, Renishaw Corporation, Britain). The absorbency of these TiO_2 film electrodes was tested by UV–vis-near-infrared spectrophotometer (UVS; Cary 500; Varian, Inc.; USA) with an integral ball (110 mm). The technical parameters of test were: the wavelength range: 200–800 nm; the wavelength accuracy: UV–vis: ±0.1 nm; wavelength reproducibility: UV–vis: <0.025 nm; resolution: UV–vis: <0.05 nm (λ: D2 656.1 nm). The BET-specific surface areas of these films were tested by surface area and porosimetry analyzer (ASAP 2010 M+C; Micromeritics Inc., USA).

2.3. Photocurrent measurement and degradation experiments

The sketch diagram of experimental device for PEC oxidative degradation reaction was shown in Fig. 1. The size of quartz container was 880 mm in length, 880 mm in highness and 30 mm in width. An aquarium air-pump was connected to the tube to provide oxygen and stir the solution. Saturated calomel electrode (SCE) and platinum foil electrode were served as reference electrode and counter electrode, respectively. An 8 W UV lamp (maximum UV irradiation peak at 253.7 nm) was employed as the excitation source and fixed 1 cm away from the quartz container. The absorbency of the Reactive Brilliant Red (RBR; Fig. 2, the molecular structure of RBR) dye solution was tested by UV–vis spectrophotometer at the wavelength of 538 nm (the maximum absorbance wavelength of RBR dye solution). The Chemical Oxygen Demand (COD) of the RBR

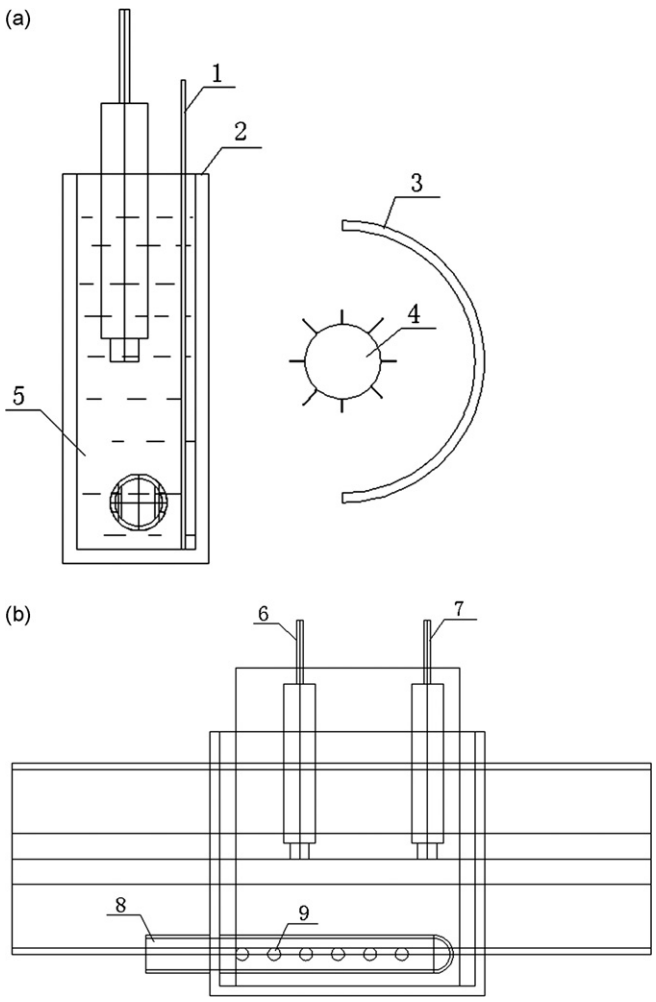

Fig. 1. (a) Schematic diagram of the side view of the TiO_2/Ti film PEC reactor: (1) TiO_2/Ti electrode; (2) quartz container; (3) aluminum foil; (4) UV lamp; (5) sample solution. (b) The front view of the TiO_2/Ti PEC reactor: (6) reference electrode; (7) counter electrode; (8) tube; (9) blowhole.

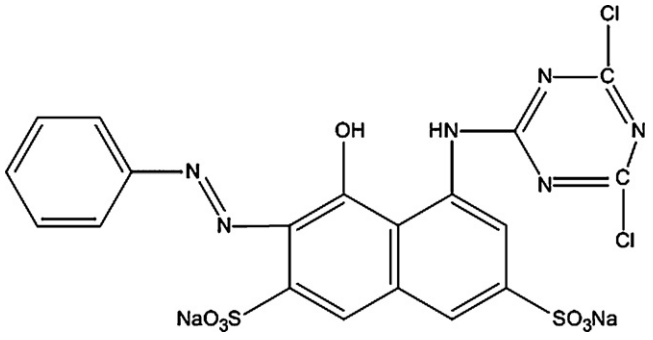

Fig. 2. The molecular structure of RBR.

dye solution was also measured by COD standard method. For accumulating the separation of photo-generated electron–hole pairs, the voltage was applied between the TiO_2/Ti film electrode and the counter electrode (the sample served as anode, the counter electrode served as cathode).

Photocurrent of the coral structure TiO_2/Ti film electrode was tested in the experimental device, as shown in Fig. 1. Electrochemical workstation (CHI660C; Chenhua; China) was employed to provide the potential and measure the current. The photocurrent was measured in 100 mL Na_2SO_4 solution (0.05 M/L). The other conditions were the same as the degradation experiments.

3. Results and discussion

3.1. The morphology and crystal structure of the TiO_2/Ti film electrodes

Fig. 3a is the surface morphology of the coral structure electrode, which shows that there are many irregular TiO_2 nanorods (about 50 nm in diameter, varying lengths) on the surface of the sample and the surface of the sample looks like coral. Due to the inhomogeneous surface stress, the titanium matrix is corroded heterogeneously during the anodic oxidation, leading to coral structure surface [30–32]. Fig. 3b is the surface morphology of the nanotube TiO_2/Ti film electrode, the size of nanotubes is about 80 nm in diameter, 10 nm in wall thickness. The formation mechanism of nanotube had been reported by Gong et al. [26]. Fig. 3c is the surface morphology of the flat film TiO_2 electrode, which shows that the surface is very flat and there are only a few micro-cracks on the surface. The presence of these micro-cracks is due to the dehydration of the gel contraction after drying treatment. The Bet-specific surface areas of nanotube, coral structure and flat TiO_2 films were 55 m^2/g, 24 m^2/g and1.4 m^2/g. It is found that that the surface area of nanotube TiO_2/Ti film electrodes is larger than that of coral structure electrode due to that nanotube has both inner surface and external surface, but the nanorod has only external surface. However owing to its scraggly surface, the surface area of the coral structure TiO_2/Ti film electrodes is larger than that of flat one.

Sclafani et al. [33] report that the anatase phase TiO_2 has a higher photocatalytic activity than that of rutile phase TiO_2. To obtain the anatase phase TiO_2 on the electrodes surface the calcination temperature is chosen at 500 °C. Fig. 4 shows the Raman spectroscopies of the three kinds of TiO_2 film electrodes. It can be seen that the Raman spectroscopies of these TiO_2 film electrodes are very similar. In the spectrum range from 100 cm^{-1} to 800 cm^{-1} there is one strong peak at 143 cm^{-1} and four weak peaks at 198 cm^{-1}, 395 cm^{-1}, 515 cm^{-1} and 638 cm^{-1}, respectively. This is the typical trait of anatase TiO_2 [34,35]. The first Raman band at 143 cm^{-1} matches the position of the first Raman band (E_g) of the TiO_2 anatase phase, and the bandwidth is quite narrow which can be explained by the growth of nanometric anatase grains [36,37]. This suggests the formation of well crystallized anatase phase and these films have a similar anatase crystal size about 42 nm which was calculated by the method mentioned in the literature [37]. The Raman band at 198 cm^{-1}, 395 cm^{-1}, 515 cm^{-1} and 638 cm^{-1} match the E_g, B_{1g}, A_{1g} and E_g Raman band of the TiO_2 anatase phase, respectively [36]. No signal associated to the rutile phase is detected.

3.2. The absorbance of the TiO_2 film electrodes

The UV–vis absorption spectroscopy of TiO_2 film electrodes is tested by UV–vis-near-infrared spectrophotometer with an integral ball, and the results are shown in Fig. 5. It can be seen that the coral structure TiO_2/Ti film not only has a strong UV absorption rate of about 87–93% but also has a strong visible light absorption rate of

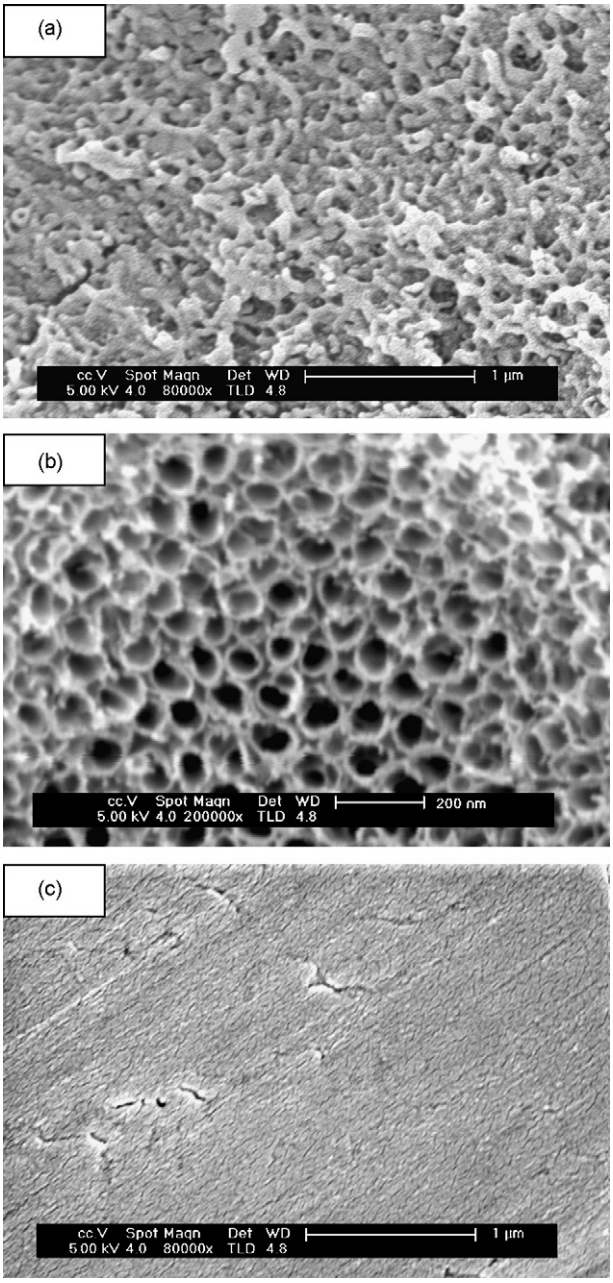

Fig. 3. SEM images of (a) the coral structure TiO_2/Ti film electrode surface; (b) the flat TiO_2 film electrode surface; (c) the nanotube TiO_2/Ti film electrode surface.

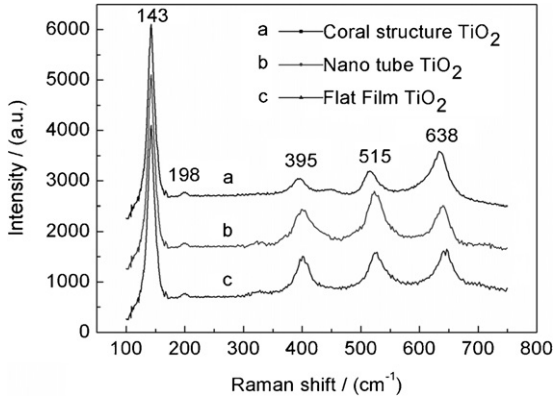

Fig. 4. Raman spectra of the coral structure, nanotube and flat TiO_2 film electrodes.

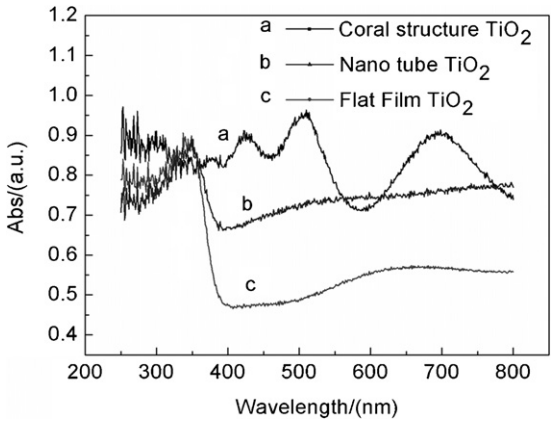

Fig. 5. UV–vis absorption spectra of the coral structure, nanotube and flat TiO_2 film electrodes.

about 77–87%. This indicates that this coral structure demonstrates good light trapping performance. When light irradiates on the surface it will be reflected back and forth several times on the surface of this structure, which results in high light absorption rate. The nanotube TiO_2/Ti film has a strong UV absorption rate of about 80–85% while has a low visible light absorption rate of about 70–75%, which indicates that the light trapping effect of nanotube is weaker than that of coral structure. The flat TiO_2 film has a strong UV absorption rate of about 75–85% but has a low visible light absorption rate of about 45–55%, which indicates that there is no effect of light trapping on flat TiO_2 film. The experimental results suggest that coral structure can enhance the rate of optical absorption and subsequently will result in the improvement of the PEC activity of the TiO_2 film by increasing the efficiency of optical utilization.

3.3. PEC experiment

The effect of applied potential on photocurrent density is shown in Fig. 6. It shows that, in the darkness, the current densities of these electrodes are very low when the potential between −0.3 V and 2 V, and increase gradually when the potential is over 2 V, which is the typical characteristic of a semiconductor [38]. When the applied potential increases over 2 V, a large number of hydrogen bubbles emerging from the solution are observed. In the experiment subsequently the dark current density is increased dramatically, which indicates that the over-high applied potential stimulates the solution to be electrolyzed. Thus, the appropriate applied potential

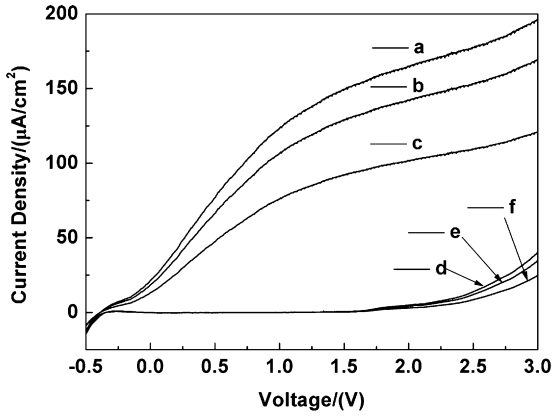

Fig. 6. Photocurrents density vs. applied bias potential curves for (a) coral structure TiO_2/Ti film electrode, (b) nanotube TiO_2/Ti film electrode, (c) flat TiO_2 film electrode at illumination and (d) coral structure TiO_2/Ti film electrode, (e) nanotube TiO_2/Ti film electrode, and (f) flat TiO_2 film electrode in darkness.

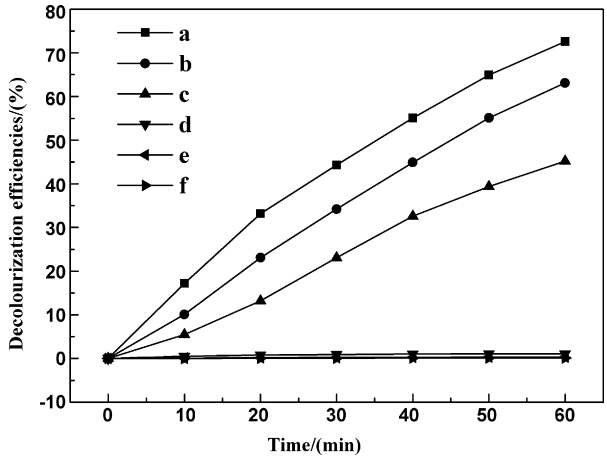

Fig. 7. Decolorization efficiencies vs. time curves for (a) coral structure TiO_2/Ti film electrode, (b) nanotube TiO_2/Ti film electrode, (c) flat TiO_2 film electrode at illumination and (d) coral structure TiO_2/Ti film electrode, (e) nanotube TiO_2/Ti film electrode, and (f) flat TiO_2 film electrode in darkness.

should be about 2 V. Under UV illumination, the photocurrent densities of these electrodes are increased rapidly at the beginning and slow down gradually. This indicates that the photo-generated electron–hole pairs are well separated by applied potential, and the increasing voltage can improve the effect of separation. This phenomenon agrees well with the results reported by Ward and Bard [27]. The photocurrent density of coral structure TiO_2/Ti film electrode is higher than those of nanotube and flat TiO_2 film electrodes at the same applied potential. When the applied potential is 2 V, the photocurrent density is about 160 $\mu A/cm^2$, 140 $\mu A/cm^2$ and 100 $\mu A/cm^2$ for the coral structure, nanotube and flat TiO_2 film electrodes, respectively.

The PEC degradation of RBR experiments by coral structure, nanotube and flat TiO_2 film electrodes were conducted in the same condition. The concentration of RBR is 30 mg/L, and the applied potential is 2 V. The effect of structure on color removal efficiency of RBR as shown in Fig. 7 indicates that, in the darkness, the color removal efficiency of RBR is very low, whatever which electrode is used. This indicates that both electrolysis and adsorption are no contributions to color removal efficiency. Under UV illumination, the color removal efficiency of RBR rises as the time increases. In an hour, the color removal efficiency of RBR achieves 73%, 63% and 45% using coral structure, nanotube and flat TiO_2 film electrodes, respectively. The coral structure TiO_2/Ti film electrode achieves the best color removal efficiency of RBR in the three electrodes. While the flat film TiO_2 electrode gets the worst color removal efficiency of RBR in the three electrodes. The effect of structure on COD removal efficiency of RBR is shown in Fig. 8. In an hour, the COD removal efficiency of RBR achieves 60%, 38% and 28% using coral structure, nanotube and flat TiO_2 film electrodes, respectively. The same conclusion can be drawn from the result of COD removal efficiency experiment that the PEC activity of coral structure TiO_2/Ti film electrode is the highest in these three electrodes. Since the crystal structure and crystal size of these three electrodes are the same, this PEC activity difference can be ascribed to the surface morphology differences of these electrodes. The coral structure TiO_2/Ti film electrode has a light trapping structure which may absorb more light than the flat TiO_2 film electrode in the same size of areas which the TiO_2 is deposited. The photoabsorbance test has proved this. High photoabsorbance means that the high photo-conversion efficiency. Besides, the coral structure and nanotube TiO_2/Ti film electrodes have larger surface areas than that of the flat TiO_2 film electrode. It increases the chance of a RBR molecule to meet a photo-generating

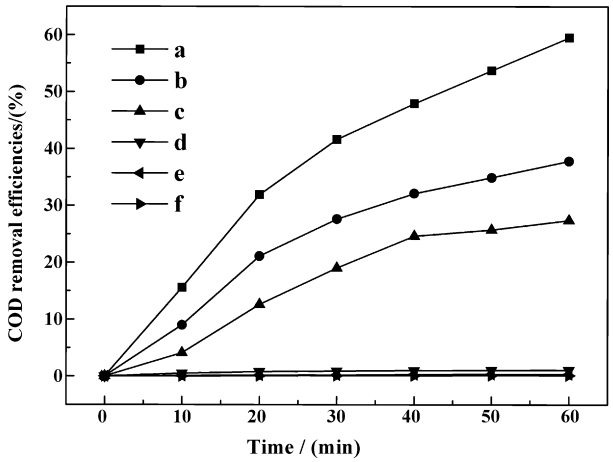

Fig. 8. COD removal efficiencies vs. time curves for (a) coral structure TiO_2/Ti film electrode, (b) nanotube TiO_2/Ti film electrode, (c) flat TiO_2 film electrode at illumination and (d) coral structure TiO_2/Ti film electrode, (e) nanotube TiO_2/Ti film electrode, and (f) flat TiO_2 film electrode in darkness.

hole on the electrode surface. Although the surface area of nanotube TiO_2/Ti film electrode is larger than that of the coral structure TiO_2/Ti film electrode, the color and COD removal efficiencies of RBR of nanotube TiO_2/Ti film electrode are less than that of the coral structure TiO_2/Ti film electrode. The surface morphology of coral structure TiO_2/Ti film electrode is an open architecture as is opposed to that of the nanotube one which is a blind pore structure, as shown in Fig. 2b. The mass transfer is testified to be much easier for an open architecture than for a blind pore structure [39]. Excellent mass transfer is supposed not only to accelerate the reaction between RBR molecules and the photo-generating holes but also to reduce the recombination of electrons with holes. Subsequently, it is expected that the utilization rate of photo-generating electrons and holes is to be improved resulting in the increasing of PEC activated.

4. Conclusion

In this study a novel coral structure TiO_2/Ti film electrode was prepared by anodic oxidation technique on the titanium matrix. The crystal structure of these TiO_2 film electrodes used for PEC experiment is anatase. The Bet-specific surface areas of nanotube, coral structure and flat TiO_2 films were 55 m^2/g, 24 m^2/g and 1.4 m^2/g. The absorbance is 87–93%, 80–85% and 75–85% in the UV light region and 77–87%, 70–75% and 45–55% in the visible light region for coral structure, nanotube and flat TiO_2 film electrodes, respectively. The photocurrent densities of these three kinds of electrodes are increased by the increase of applied potential. At the application potential of 2 V, the photocurrent density is about 160 $\mu A/cm^2$, 140 $\mu A/cm^2$ and 100 $\mu A/cm^2$ for the coral structure, nanotube and flat TiO_2 film electrodes, respectively. The color removal efficiency of RBR, in an hour, achieves to 73%, 63% and 45% when using coral structure, nanotube and flat TiO_2 film electrodes, respectively. Although the surface area of coral structure TiO_2/Ti film electrode is less than that of nanotube TiO_2/Ti film electrode, the color and COD removal efficiencies of coral structure TiO_2/Ti film electrode are 16%, 58% higher than these of nanotube TiO_2/Ti film electrodes, respectively. The improvements of photocurrent density and the color removal efficiency of coral structure TiO_2/Ti film electrode are ascribed to increase of light absorbance caused by light trapping effect and to decrease of electron–hole pair recombination owing to the better mass transmission through this kind of open architecture.

References

[1] W.J. Epolito, H. Yang, L.A. Bottomley, S.G. Pavlostathis, Kinetics of zero-valent iron reductive transformation of the anthraquinone dye Reactive Blue 4, J. Hazard. Mater. 160 (2008) 594–600.
[2] Y.M. Dong, K. He, B. Zhao, Y. Yin, L. Yin, A. Zhang, Catalytic ozonation of azo dye active brilliant red X-3B in water with natural mineral brucite, Catal. Commun. 8 (2007) 1599–1603.
[3] I.A.W. Tan, A.L. Ahmad, B.H. Hamee, Adsorption of basic dye on high-surface-area activated carbon prepared from coconut husk: equilibrium, kinetic and thermodynamic studies, J. Hazard. Mater. 154 (2008) 337–346.
[4] M.A. Behnajady, N. Modirshahla, F. Ghanbary, A kinetic model for the decolorization of C.I. Acid Yellow 23 by Fenton process, J. Hazard. Mater. 48 (2007) 98–102.
[5] M. Mahbubul Hassan, C.J. Hawkyard, Ferral-catalyzed ozonation of aqueous dyes in a bubble-column reactor, Catal. Commun. 3 (2002) 281–286.
[6] D.E. Kritikos, N.P. Xekoukoulotakis, E. Psillakis, D. Mantzavinos, Photocatalytic degradation of reactive black 5 in aqueous solutions: effect of operating conditions and coupling with ultrasound irradiation, Water Res. 41 (2007) 2236–2246.
[7] M. Faisal, M. Abu Tariq, M. Muneer, Photocatalysed degradation of two selected dyes in UV-irradiated aqueous suspensions of titania, Dyes Pigments 72 (2007) 233–239.
[8] H. Zhang, L.J. Duan, D.B. Zhang, Decolorization of methyl orange by ozonation in combination with ultrasonic irradiation, J. Hazard. Mater. 138 (2006) 53–59.
[9] R. Jain, S. Varshney, S. Sikarwar, Electrochemical techniques for the removal of Reactofix Golden Yellow 3 RFN from industrial wastes, J. Colloid Interface Sci. 313 (2007) 248–253.
[10] A. Fujishima, K. Honda, Electrochemical photolysis of water at a semiconductor electrode, Nature 238 (1972) 37–38.
[11] G.M. Liu, X.Z. Li, J.C. Zhao, H. Hiadaka, N. Serpone, Photooxidation pathway of sulforhodamine-B dependence on the adsorption mode on TiO_2 exposed to visible light radiation, Environ. Sci. Technol. 34 (2000) 3982–3990.
[12] D.K. Lee, I.C. Cho, Characterization of TiO_2 thin film immobilized on glass tube and its application to PCE photocatalytic destruction, Microchem. J. 68 (2001) 215–223.
[13] P.S. Marcos, J. Marto, Screen-printing of TiO_2 photocatalytic layers on glazed ceramic tiles, J. Photochem. Photobiol. A 197 (2008) 125–131.
[14] S. Yoda, Y. Tasaka, TiO_2-impregnated SiO_2 aerogels by alcohol supercritical drying with zeolite, J. Non-Cryst. Solids 225 (1998) 105–110.
[15] C. He, Y. Xiong, D. Shu, X.H. Zhu, X.Z. Li, Preparation and photoelectrocatalytic activity of Pt (TiO_2)–TiO_2 hybrid films, Thin Solid Films 503 (2006) 1–7.
[16] J.J. Sene, W.A. Zeltner, M.A. Anderson, Fundamental photoelectrocatalytic and electrophoretic mobility studies of TiO_2 and V-doped TiO_2 thin-film electrode materials, J. Phys. Chem. B 107 (2003) 1597–1603.
[17] H.J. Sayılkan, Improved photocatalytic activity of Sn^{4+} doped and undoped TiO_2 thin film coated stainless steel under UV- and VIS-irradiation, Appl. Catal. A 319 (2007) 230–236.
[18] T.A. Egerton, M. Janus, A.W. Morawski, New TiO_2/C sol–gel electrodes for photoelectrocatalytic degradation of sodium oxalate, Chemosphere 63 (2006) 1203–1208.
[19] R.S. Manea, S.J. Roha, O.S. Joob, C.D. Lokhandec, S.H. Hana, Improved performance of dense TiO_2/CdSe coupled thin films by low temperature process, Electrochim. Acta 50 (2005) 2453–2459.
[20] D.H. Kim, M.A. Anderson, Photoelectrocatalytic degradation of formic acid using a porous TiO_2 thin-film electrode, Environ. Sci. Technol. 28 (1994) 479–483.
[21] X.Z. Li, F.B. Li, C.M. Fang, Y.P. Sun, Photoelectrocatalytic degradation of humic acid in aqueous solution using a Ti/TiO_2 mesh photoelectrode, Water Res. 36 (2002) 2215–2224.
[22] D.L. Jiang, H.J. Zhao, S.Q. Zhang, R. John, Characterization of photoelectrocatalytic processes at nanoporous TiO_2 film electrodes: photocatalytic oxidation of glucose, J. Phys. Chem. B 107 (2003) 12774–12780.
[23] H. Selcuk, J.J. Sene, M.V.B. Zanoni, H.Z. Sarikaya, M.A. Anderson, Behavior of bromide in the photoelectrocatalytic process and bromine generation using nanoporous titanium dioxide thin-film electrodes, Chemosphere 54 (2004) 969–974.
[24] X.Z. Li, H.L. Liu, P.T. Yue, Photoelectrocatalytic oxidation of Rose Bengal in aqueous solution using a Ti/TiO_2 mesh electrode, Environ. Sci. Technol. 34 (2000) 4401–4406.
[25] P.A. Carneiro, M.E. Osugi, J.J. Sene, Evaluation of color removal and degradation of a reactive textile azo dye on nanoporous TiO_2 thin-film electrodes, Electrochim. Acta 49 (2004) 3807–3820.
[26] D.W. Gong, C.A. Grimes, O.K. Varghese, W.C. Hu, R.S. Singh, Z. Chen, E.C. Dickey, Titanium oxide nanotube arrays prepared by anodic oxidation, J. Mater Res. 16 (2001) 3331–3334.
[27] M.D. Ward, A.J. Bard, Photocurrent enhancement via trapping of photogenerated electrons of titanium dioxide particles, J. Phys. Chem. 86 (1982) 3599–3605.
[28] N.K. Kuromoto, R.A. Simao, G.A. Soares, Titanium oxide films produced on commercially pure titanium by anodic oxidation with different voltages, Mater. Charact. 58 (2007) 114–121.
[29] M.V.B. Zanoni, Photoelectrocatalytic degradation of remazol brilliant orange 3R on titanium dioxide thin-film electrodes, J. Photochem. Photobiol. A: Chem. 157 (2003) 55–63.
[30] W.A. Tiller, S. Ciraci, I.P. Batra, Some effects of inhomogeneous strain on surface properties of metals. I. Flat surface, Surf. Sci. 65 (1977) 173–188.

[31] H. Miyamoto, K. Harada, Corrosion of ultra-fine grained copper fabricated by equal-channel angular pressing, Corros. Sci. 50 (2008) 1215–1220.
[32] Y.N. Ivashchenko, N.V. Vyazovikina, Structure effect on corrosion failure in iron-chromium alloys, Mater. Sci. 28 (1993) 363–367.
[33] A. Sclafani, L. Palmisano, M. Schiavello, Influence of the preparation methods of titanium dioxide on the photocatalytic degradation of phenol in aqueous dispersion, J. Phys. chem. 94 (1990) 829–832.
[34] S. Boukrouh, R. Bensaha, Reactive direct current magnetron sputtered TiO_2 thin films with amorphous to crystalline structures, Thin Solid Films 516 (2008) 6353–6358.
[35] T. Ohsaka, F. Izumi, Y. Fujiki, Raman spectrum of anatase, TiO_2, J. Raman Spectrosc. 7 (1978) 321–324.
[36] W.F. Zhang, Y.L. He, M.S. Zhang, Z. Yin, Q. Chen, Raman scattering study on anatase TiO_2 nanocrystals, J. Phys. D: Appl. Phys. 33 (2000) 912–916.
[37] C. Pighini, D. Aymes, N. Millot, L. Saviot, Low-frequency Raman characterization of size-controlled anatase TiO_2 nanopowders prepared by continuous hydrothermal syntheses, J. Nanoparticle Res. 9 (2007) 309–315.
[38] M.D. Earle, The electrical conductivity of titanium dioxide, Phys. Rev. 61 (1942) 56–62.
[39] R. Ash, R.W. Baker, R.M. Barrer, Sorption and surface flow in graphitized carbon membranes II. Time-lag and blind pore character, Proc. R. Soc. Lond. A: Math. Phys. Sci. 304 (1968) 407–425.